Meteorol Atmos Phys
DOI 10.1007/s00703-011-0179-z

ORIGINAL PAPER

An evaluation of air quality modeling over the Pearl River Delta during November 2006

Qizhong Wu · Zifa Wang · Huansheng Chen · Wen Zhou · Mark Wenig

Received: 10 August 2011 / Accepted: 23 December 2011

Abstract In this paper, we evaluate the performance of several air quality models using the Pearl River Delta (PRD) region, including the Nested Air Quality Prediction Modeling System (NAQPMS), the Community Multiscale Air Quality (CMAQ) model, and the Comprehensive Air Quality Model with extensions (CAMx). All three model runs are based on the same meteorological fields generated by the Fifth-Generation Pennsylvania State University/National Center for Atmospheric Research (PSU/NCAR) Mesoscale Model (MM5) and the same emission inventories. The emission data are processed by the Sparse Matrix Operator Kernel Emissions (SMOKE) model, with the inventories generated from the Transport and Chemical Evolution over the Pacific/Intercontinental Chemical Transport ExperimentPhase B (TRACE-P/INTEX-B) and local emission inventory data. The results show that: (1) the meteorological simulation of the MM5 model is reasonable compared with the observations at the regional background and urban stations. (2) The models have different advantages at different stations. The CAMx model has the best performance for SO_2 simulation, with the lowest mean normalized bias (MNB) and mean normalized error (MNE) at most of the Guangzhou stations, while the CMAQ model has the lowest normalized mean square error (NMSE) value for SO_2 simulation at most of the other PRD urban stations. The NAQPMS model has the best performance in the NO_2 simulation at most of the Guangzhou stations. (3) The model performance at the Guangzhou stations is better than that at the other stations, and the emissions may be underestimated in the other PRD cities. (4) The PM_{10} simulation has the best model measures of FAC2 (fraction of predictions within a factor of two of the observations) (average 53–56%) and NMSE (0.904–1.015), while the SO_2 simulation has the best concentration distribution compared with the observations, according to the quantile–quantile (Q–Q) plots.

Responsible editor: S. Trini Castelli.

Electronic supplementary material The online version of this article (doi:10.1007/s00703-011-0179-z) contains supplementary material, which is available to authorized users.

Q. Wu
College of Global Change and Earth System Science, Beijing Normal University, Beijing, China

Q. Wu · W. Zhou (✉) · M. Wenig
Guy Carpenter Asia–Pacific Climate Impact Center, School of Energy and Environment, City University of Hong Kong, Hong Kong, China
e-mail: wenzhou@cityu.edu.hk

Z. Wang · H. Chen
LAPC, Institute of Atmospheric Physics, Chinese Academy of Sciences, Beijing, China

H. Chen
Graduate University of Chinese Academy of Sciences, Beijing, China

1 Introduction

The Pearl River Delta (PRD) is a highly urbanized area containing two megacities (Guangzhou and Hong Kong) and numerous medium-sized cities, including Shenzhen, Foshan, Dongguan, and others. Rapid urbanization causes significant air quality deterioration, such as heavy air pollutants and low visibility (Chan and Yao 2008; Deng et al. 2008). During the Program of Regional Integrated Experiments on Air Quality over the Pearl River Delta of China in October 2004 (PRIDE-PRD2004), the PM_{10} concentration reached as high as 363 μg/m^3 and SO_2 was up to

Published online: 24 January 2012

187 ppbv, while NO_2 was up to 144 ppbv (Wang et al. 2008; Zhang et al. 2008). Because of its adverse effects on health and the environment, air pollution has become a focus for research in recent years. In order to understand the chemical and radiative processes, provide accurate air quality data, and appraise the air quality situation in the PRD region, the Pearl River Delta Regional Air Quality Monitoring (PRD-RAQM) Network was jointly established by the Guangdong Provincial Environmental Protection Monitoring Centre (GDEMC) and the Environmental Protection Department of the Hong Kong Special Administrative Region (HKEPD; GDEMC and HKEPD 2009).

Air quality models play an important role not only in science, but also for policy decisions, since they can provide scientific advice for air pollution control measures (Wang et al. 2005, 2009a; Feng et al. 2007). Wang et al. (2009a) used the Weather Research and Forecasting model coupled with Chemistry (WRF-Chem) model to explore the impacts of urban expansion on regional weather conditions and its implication for surface ozone concentrations, and the results showed that urbanization increases surface ozone concentrations. Chen et al. (2009) used the Fifth-Generation Pennsylvania State University/National Center for Atmospheric Research (PSU/NCAR) Mesoscale Model/Community Multiscale Air Quality (MM5-CMAQ) model system to investigate atmospheric haze and concluded that land breezes can transport PM_{10} to the coast and the sea at night, and sea breezes can carry the accumulated offshore PM_{10} back to inland cities in the daytime. Most model studies have focused on reproducing typical high air pollutant episodes and have run experimental scenarios with different emissions. The performance of each model cannot be compared directly with the PRD region, but over the eastern US, operational and comparative evaluations of the CMAQ and Comprehensive Air Quality Model with extensions (CAMx) models have been performed (Tesche et al. 2006).

The air quality ensemble multimodel system has been developed and used in science and operational forecasting (Wang et al. 2009b; Wu et al. 2010a). In this paper, we evaluate the model performance of each ensemble member model using the same meteorological driver and emissions, the results of which may be used to: (a) clarify the uncertainty in model estimates for SO_2, NO_2, and PM_{10} in the PRD region; and (b) improve data input preparation procedures, such as emissions.

2 Methodology and data

There are three air quality models used in the ensemble multimodel system (Fig. 1): the Nested Air Quality Prediction Modeling System (NAQPMS) version 3.3 model from the Institute of Atmospheric Physics, Chinese Academy of Sciences; the CMAQ version 4.4 model system (Byun and Ching 1999; Byun and Schere 2006) from the US Environmental Protection Agency; and the CAMx version 4.4 model (ENVIRON 2002) from the US Environ Corporation. The same meteorological fields are generated by the MM5 version 3.6 model (Grell et al. 1994), and the same emissions are processed by the Sparse Matrix Operator Kernel Emissions (SMOKE) version 2.3 model.

2.1 Meteorological field

The MM5 model is used to generate the unique meteorological field for the air quality models. The National Centers for Environmental Prediction (NCEP) global final analysis data (FNL), with $1^\circ \times 1^\circ$ resolution and a frequency of four times a day, is used as the initial and boundary conditions for the regional meteorological model MM5. Also chosen are certain parameterization schemes, including simple ice for explicit moisture schemes, Grell cumulus schemes, MRF for PBL schemes, and cloud schemes for atmospheric radiation. According to the results of Colle et al. (1999) and Lo et al. (2007), if the MM5 simulations are initialized with a cold start, it might take at least 12 h on average for the model to spin up. We perform our meteorological simulations for the period of 1–30 November 2006 using the predicting cycle method, making 36-h simulations, taking the last 24-h simulation as the meteorological driver in every predicting cycle, and linking the meteorological simulations for 1 month.

2.2 Air quality model descriptions

The NAQPMS model is a three-dimensional chemical transport model with various options for representing physical and chemical processes for regional- and urban-scale atmospheric pollution, and it has been applied to study the mechanisms of air pollutants and dust events in East Asia (Huang et al. 1995; Wang et al. 2001, 2006a; Li et al. 2007; Wu et al. 2010b). The chemical transport module solves the mass balance equation in terrain-following coordinates, and its gas-phase chemistry mechanism has been updated to CBM-Z (Zaveri and Peters 1999) by Li et al. (2007). More details can be found in Wang et al. (2000, 2002, 2006b, 2011).

The CMAQ model is used for regional- and urban-scale air quality simulations of tropospheric ozone, acid deposition, visibility, and particulate matter (Byun and Ching 1999), and has already been widely used all over the world, including East Asia (An et al. 2007; Cheng et al. 2007; Zhang et al. 2006). It contains state-of-the-art parameterizations of atmospheric processes affecting transport, transformation, and wet/dry deposition. The CB-IV scheme

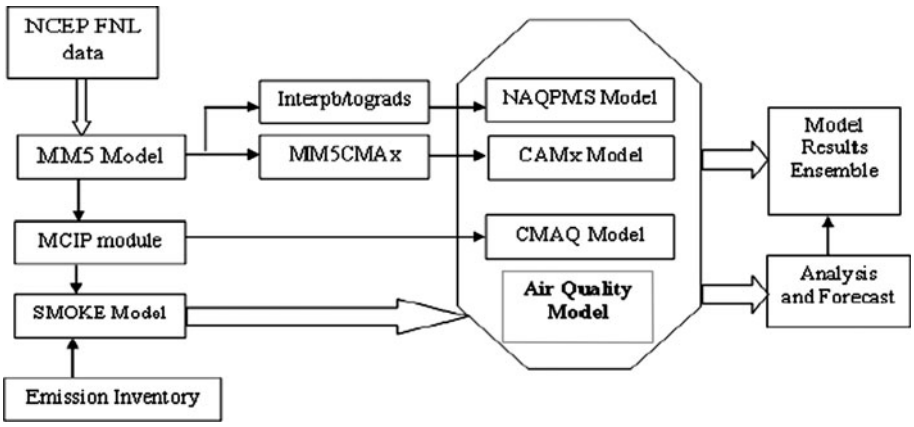

Fig. 1 The framework of the air quality multimodel system (Wang et al. 2009b)

(Gery et al. 1989) for gas-phase chemistry and the AERO3 module for aerosol calculation (Binkowski and Roselle 2003) are applied in this study. The photolysis rate model (JPROC) is used to calculate the day-specific clear sky photolysis rate look-up table for latitudinal and elevation bands for each photochemical reaction in the gas-phase chemistry, based on work published by Demerjian et al.'s (1980) scheme (Cruickshank 2008).

The CAMx model is also a three-dimensional Eulerian tropospheric photochemical dispersion model that allows for integrated "one-atmosphere" assessments of gaseous and particulate air pollution at continental and suburban scales. The CB-IV gas-phase chemistry with additional inorganic reactions for aerosol calculation is used in this study. The Tropospheric Ultra-violet Visible (TUV) model (Madronich 2002), which is developed by the NCAR, is used to provide a multidimensional look-up table of photolysis rates. For further description of the CMAQ and CAMx models, see Byun and Ching (1999) and ENVIRON (2002).

In this study, the NAQPMS, CMAQ, and CAMx models are extensively evaluated using a 1-month-long episode (November 2006), with the final scientific configurations (see Table 1) used for the first performance evaluations.

2.3 Model setup and configuration

The four nested domains (Fig. 2), with the center located at 25.5°N, 112°E, and the two true latitudes of 10°N and 40°N, are used for the NAQPMS and CMAQ models, and the inner two domains (GZ09 and GZ03) are used for the CAMx model. The boundary condition of the outermost domain (GZ81) of the NAQPMS and CMAQ models is a clean boundary field, while the boundary condition of the CAMx model in the GZ09 domain is generated from the CMAQ model results in the GZ27 domain. Thus, the CMAQ and CAMx models in the GZ09/GZ03 domain simulations share the same boundary conditions. The NAQPMS and CAMx models use a two-way nested method for the simulation, while the CMAQ model uses a one-way nested method.

There are 23 sigma vertical layers unequally distributed in the MM5 model, with the top layers at 10 hPa and six layers below 1 km. The CMAQ and CAMx models have 14 vertical layers, with the ten lowest layers the same as the MM5 model, but the NAQPMS model has 20 vertical layers extending from 1,000 to 100 hPa. The height of the surface (lowest) layer is approximately 35 m.

Clean initial conditions are used, the influence of which will decrease while the simulation proceeds and will eventually be lost (Seinfeld and Pandis 1998). Thus, the initial conditions are based on clean-troposphere vertical profile concentration fields at the beginning of a simulation, and the first 24 h of results are used for spin-up.

2.4 Emissions process

The SMOKE model is applied to deal with the same emissions inventory and provide gridded emissions data for the air quality models. We deal with the emissions as area/point sources: the area source emissions take a "top-down" approach, giving a total emission and assigning the emission to grid cells with relative spatial distribution factors such as population, road density, etc.; the point source emissions are put into the model grid based on their longitude–latitude position, and the stack parameters, such as stack height, diameter, and exit gas temperature are used for computing the hourly plume rise with the meteorological parameters from the MM5 model results with the MCIP module (Houyoux and Vukovich 1999). The mobile and biogenic sources are handled as area source emissions.

Three emission inventories are used in this study: the regional emissions in East Asia from Transport and Chemical Evolution over the Pacific (TRACE-P) without power plant emissions (Streets et al. 2003, 2006); the Intercontinental Chemical Transport ExperimentPhase B (INTEX-B) power plant emissions inventory with 30-min resolution (Zhang et al. 2009); and the local emission

Table 1 The air quality model configurations

Model	NAQPMS[a]	CMAQ[b]	CAMx[c]
Model version	Version 3.3	Version 4.4	Version 4
Horizontal resolution	81/27/9/3 km	81/27/9/3 km	9/3 km
Grid nesting	Two-way	One-way	Two-way
Vertical layers	20 layers	14 layers	14 layers
Horizontal advection	Walcek and Aleksic (1998)	PPM	PPM
Vertical advection	Walcek and Aleksic (1998)	PPM	Implicit
Horizontal diffusion	$k_H = 45\ m^2s^{-1}$	Spatially varying	Spatially varying
Vertical diffusion	K_z (Eddy diff.)	K_z (Eddy diff.)	K_z (Eddy diff.)
Gas-phase mechanisms	CBM-Z	CB-IV	CB-IV
Gas-phase chemistry solver	LSODE	MEBI	CMC fast solver
Aqueous-phase mechanisms	RADM	RADM	RADM
Aerosol chemistry	–	AE3/ISORROPIA	M4/ISORROPIA
Secondary organic aerosol	–	–	SOAP[d]
Dry deposition	Padro et al. (1991)	Pleim-Xiu	Wesely
Boundary conditions	Clean	Clean	27 km CMAQ results

[a] Model description and configuration are based on Wang et al. (2006b) and Wu et al. (2011)

[b] Model configuration is based on the US Environmental Protection Agency website at http://www.epa.gov/asmdnerl/CMAQ/release44.html

[c] Model configuration is based on ENVIRON (2002)

[d] Secondary organic aerosol formation/partitioning (SOAP), with reference to Strader et al. (1999)

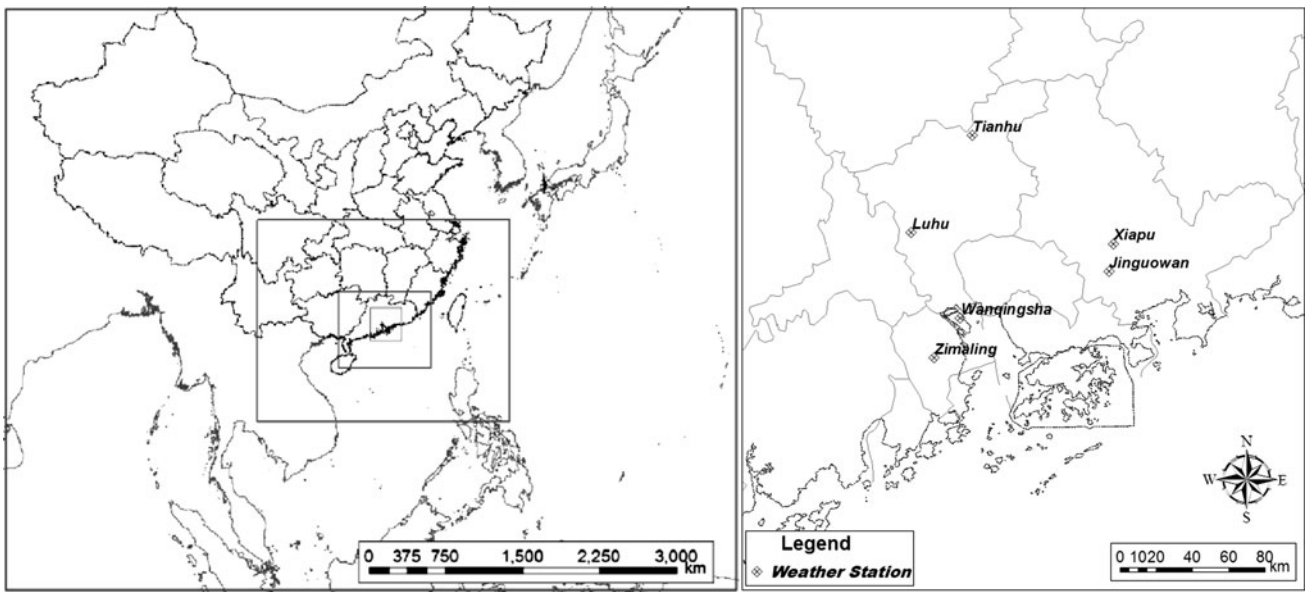

Fig. 2 The four nested domains used for simulation. D4 (GZ03) is magnified on the right. D1 (GZ81) covers East Asia with 91 × 73 grid cells at a horizontal resolution of 81 km; D2 (GZ27) with 94 × 76 grid cells includes South China; D3 (GZ09) with 103 × 85 grid cells covers the whole Guangdong Province and Hong Kong; D4 with 106 × 109 grid cells consists of Guangzhou and its surrounding cities in the Pearl River Delta (PRD) region

inventory covering the PRD region. The 6-min resolution TRACE-P emissions are handled as area sources, and the INTEX-B power plant is taken as a large point source and replaces the power plant emission in TRACE-P. The local emission inventory includes two parts. One is provided from the Asian Games Air Quality Project Group; the emissions cover the PRD cities in Guangdong Province (Table 2), including transport, residential, unorganized industrial, and road dust area source emissions, as well as power plant and industrial point source emissions. More details about the emission inventory can be found in Zheng et al. (2009). The second part is provided by the HKEPD

and includes industrial and residential point sources in Hong Kong and Macau. The gridded emissions for the models are shown in Fig. 3.

2.5 Observations for model evaluation

Observations collected by the PRD-RAQM Network and the Guangzhou Air Quality Monitoring (GZ-AQM) Network are used to evaluate model performance. The station locations are shown in Fig. 4; most GZ-AQM Network stations are located in urban areas, while the regional background stations Tianhu and HZjinguowan are located at the northern and eastern edges of the PRD region, respectively, and the Wanqingsha station is located in the estuary of the Pearl River, near the sea (GDEMC and HKEPD 2007). All stations measure the ambient concentrations of SO_2, NO_2, and PM_{10}. The design and operation of the network comply with the requirements set out in the QA/QC operating procedures. The control limits adopted for the gaseous pollutants and PM_{10} are ± 20 and $\pm 10\%$, respectively (GDEMC and HKEPD 2007). Some of the PRD-RAQM stations also measure meteorological fields, and these measurements have been collected to evaluate the MM5 model results.

3 Model evaluations for meteorological fields and air pollutants

3.1 Meteorological fields

The meteorological observations in the regional background stations (Tianhu, Wanqingsha, and HZjinguowan) and the urban stations (Luhu, ZHZimaling, and HZxiapu) are used for evaluation in Table 3 and the time series plots. The correlation coefficients in both the regional background stations and the urban stations are satisfactory, with values above 0.7 illustrating that the MM5 model performs well in simulating T, P, and Rh.

The simulations match the observations quite well in Fig. 5. As shown in Table 4, the mean normalized errors (MNE) of T and P at those stations are all below 10% in our simulation. The correlation coefficients of T, P, and Rh are all above 0.7 during the month, illustrating that the MM5 model performs well in the T, P, and Rh simulations.

Wind fields may have a higher sensitivity depending on their location. The wind fields observed at the G1045 and G1048 stations in the Guangdong Automatic Weather Station Network, which are near the Luhu and Wanqingsha stations, respectively, are used for comparison with the simulations. The distances from G1045 and G1048 to Luhu and Wanqingsha stations are both about 4 km, which stands for one or two grids in the GZ03 model domain. In November, due to the winter monsoon, the wind direction is mostly north (Zhou et al. 2007a, b, 2009), and the simulated wind directions match well with the observations at both the G1045 and G1048 stations. The mean error (ME) of wind speed decreases from 3.8 m/s at Luhu to 3.0 m/s at G1045, and from 3.6 m/s at Wanqingsha to 2.5 m/s at G1048. Thus, the simulations match well with the wind field observations at the G1045 and G1048 stations.

3.2 Model evaluation for air pollutant simulation

In this section, the SO_2, NO_2, and PM_{10} are evaluated with quantile–quantile (Q–Q) plots and standard statistical measures. The Q–Q plots are provided to compare the concentration distributions between the simulations and observations. With the Q–Q plots, biases at low or high concentrations are quickly revealed (Chang and Hanna 2004). In addition, a series of statistical measures is applied to evaluate the model performance for the SO_2, NO_2, and PM_{10} concentrations, including the mean normalized bias (MNB) and the MNE.

Table 2 Emissions in Pearl River Delta (PRD) cities for 2006

City	SO_2	NOx	PM_{10}	PM_{25}	CO	VOCs
Guangzhou	160.1	266.8	214.6	92.5	1,028.7	230.1
Shenzhen	74.3	139.6	76.7	41.0	662.2	155.2
Zhuhai	42.8	43.5	29.1	13.2	104.5	34.6
Foshan	94.0	113.2	140.5	66.6	611.7	167.1
Jiangmen	55.7	100.5	122.7	55.5	312.1	132.8
Dongguan	180.2	133.4	146.8	65.9	525.5	119.5
Zhongshan	33.7	36.4	44.1	20.3	199.2	72.9
Huizhou	12.2	20.3	55.7	25.6	143.3	135.7
Zhaoqing	15.2	16.0	59.3	26.5	159.3	61.9
Qingyuan	20.8	39.9	128.3	58.9	297.8	32.2
Total	689.0	909.6	1,017.8	466.0	4,044.3	1,142.0

Unit: 10^3 tons/year

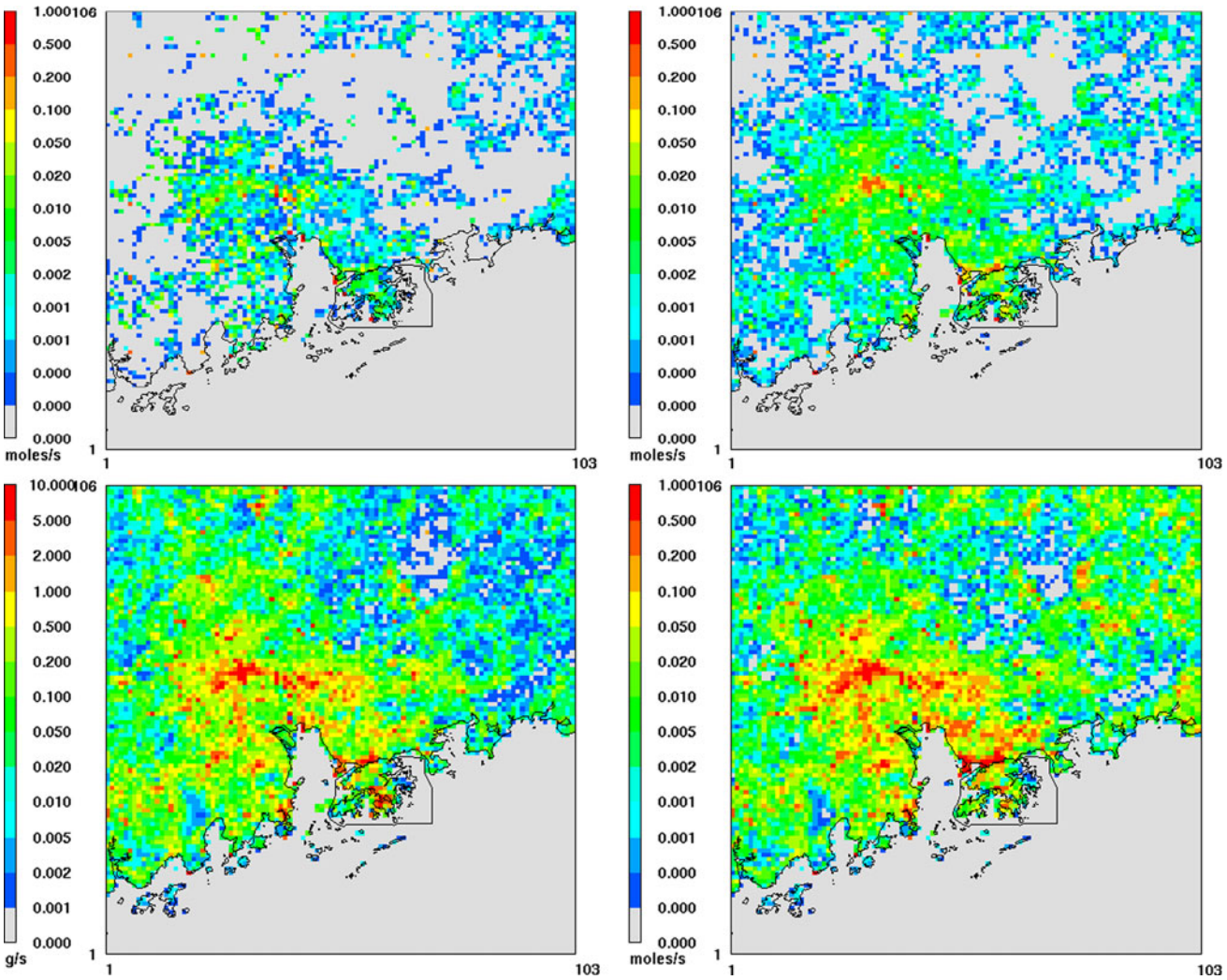

Fig. 3 Emissions of SO_2 (*upper left*), NOx (*upper right*), PM_{10} (*lower left*), and CO (*lower right*) in the model domain of GZ03 (SO_2, NOx, and CO unit: mole/s/grid; PM_{10} unit: g/s/grid)

3.2.1 Sulfur dioxide (SO_2)

Sulfur dioxide is the predominant anthropogenic sulfur-containing air pollutant (Seinfeld and Pandis 1998). It comes from the combustion of sulfur-containing fossil fuels and contributes to acid rain. The monthly average SO_2 concentration in the PRD stations reached 0.123 mg/m^3 in November 2006 in the PRD-RAQM network (GDEMC and HKEPD 2007), while the National Standard (referring to Class 2 of the National Ambient Air Quality Standard [NAAQS II]) annual SO_2 concentration was 0.060 mg/m^3. The SO_2 concentration in the PRD region is high and has become the focus of concerns over air quality.

In this study, the main air pollution episodes (8–11, 13, 16–18, and 25–27 November) have been simulated well by the models according to the time series plots in Fig. 6. But at Luhu, Jiancezhan, and Wuzhong stations, the air pollution episode of 5 November has not been simulated well by the three models, and the simulated SO_2 concentration is much lower than that observed. These stations are located in urban areas, and there is a weak north wind during this episode, which is shown in Fig. 5 for Luhu station. The SO_2 emissions in the north in the urban Guangzhou area may be underestimated because the simulation cannot reach a high concentration during the time of the weak north wind on 5 November. A more detailed evaluation of the air pollution episode of 5 November has been added in the Supplementary material 1. Thus, the simulation–observation Q–Q plots of the SO_2 concentration at these stations are below the line $y = x$, especially in the high concentration range (shown in Fig. 7). Moreover, the emissions around HuaDu station must have been underestimated, with the Q–Q plots of the three model results below the line $y = x$ for the whole concentration distribution, and the MNB of the three model SO_2 simulations ranging from -32 to -20% (Table 5).

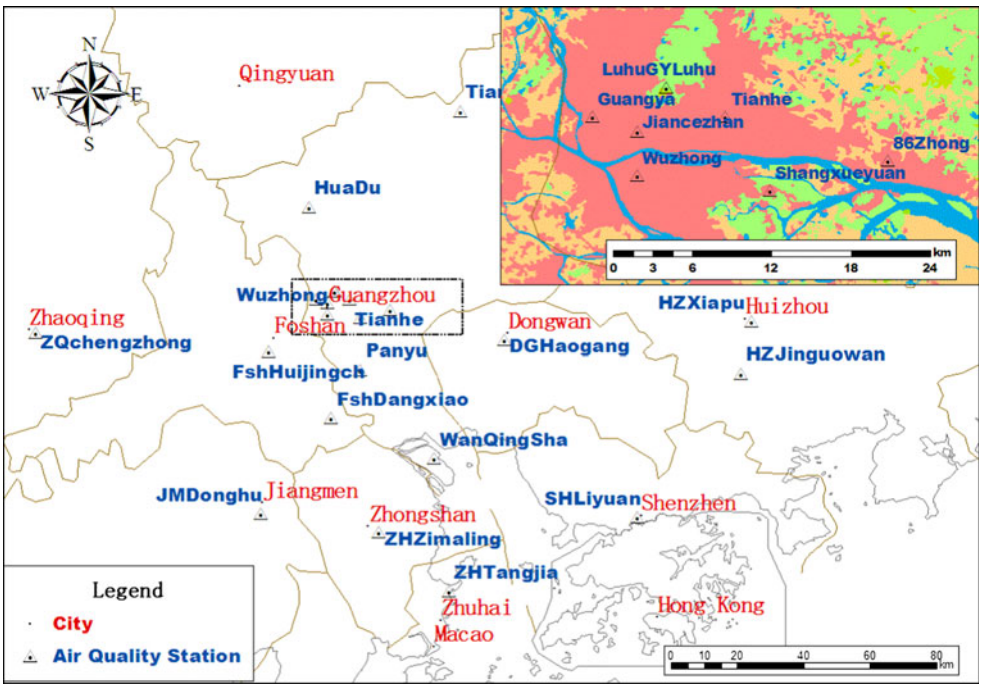

Fig. 4 The location of air quality stations for model evaluation, including 13 stations in the Pearl River Delta Regional Air Quality Monitoring (PRD-RAQM) Network (Tianhu, HZjinguowan, and Wanqingsha stations are the regional background stations) and nine stations in the Guangzhou Air Quality Monitoring (GZ-AQM) Network. The urban area of Guangzhou is magnified in the *upper right*

Table 3 Correlation coefficients (R) between observations and simulations at each station

Stations	Luhu	Zimaling	Xiapu	Tianhu	Wanqingsha	Jinguowan
T	0.74	0.75	0.79	0.79	0.74	0.73
P	0.83	0.86	0.88	0.86	0.87	0.88
Rh	0.80	0.89	0.81	0.87	0.85	0.78

Three urban stations in the surrounding cites (including FshHuijingch station to the west of Guangzhou, DGHaogang station in the southeast, and ZQchengzhong station in the northwest) are used to evaluate the model performance for the SO_2 simulation and to compare to the urban stations in Guangzhou. FshHuijingch station has the highest SO_2 concentration in the PRD region (GDEMC and HKEPD 2007) and plays an important role in Guangzhou air quality. The observed hourly SO_2 concentrations in the three urban stations are so high that they reach 600 μg/m^3 at FshHuijingch station (Fig. 6), but the simulated concentrations are much lower, with the highest simulated SO_2 concentration just reaching 400 μg/m^3 in the CMAQ results at FshHuijingch station (Fig. 7). In the Q–Q plots of FshHuijingch and DGHaogang stations, the simulated concentrations match well with the observations in the low concentration range, but are much lower in the high concentration range. The highly elevated emissions near FshHuijingch and DGHaogang stations may be underestimated, which would have a great impact on the local scale in an air pollutant episode during a weak wind condition, such as the wind condition on 5 November at FshHuijingch, shown in Fig. 8.

As mentioned above, the regional background stations Tianhu and HZjinguowan are located at the northern and eastern edges of the PRD region, respectively, and Wanqingsha station is near the sea. At Tianhu and HZJinguowan stations, the CMAQ and CAMx models results match well with the observations, except for the high episode on 10 November, according to the time series plots (Fig. 6): the high SO_2 concentration also could not be simulated well by the two models, with the highest SO_2 concentration of the CMAQ/CAMx models just reaching 100 and 80 μg/m^3 at Tianhu and HZJinguowan stations, respectively, while the observed highest SO_2 concentration reached 250 and 100 μg/m^3, respectively. Compared to the CMAQ/CAMx results, the NAQPMS model results at Tianhu and HZJinguowan stations are much lower and less accurate; in contrast, the NAQPMS model performs better than the CMAQ/CAMx models at Wanqingsha station, according to the Q–Q plots of Fig. 7 and the statistical measures in Table 6. The SO_2 simulation is controlled mainly by physical processes and aqueous-phase chemical mechanisms. The three models have the same aqueous-phase chemical mechanisms, so the differences in their SO_2 simulations are caused mostly by their physical processes.

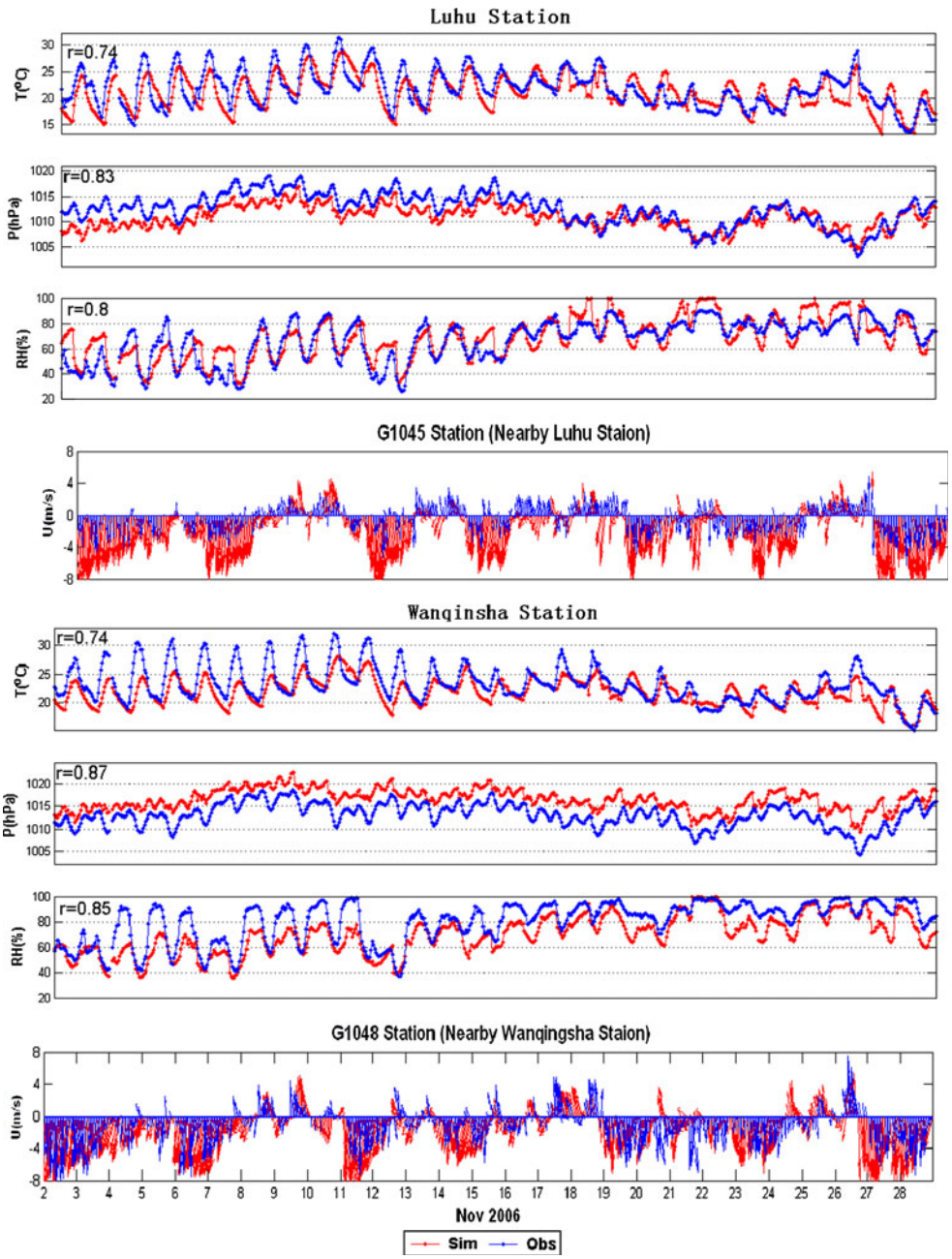

Fig. 5 Time series of the meteorological variables (temperature, pressure, relative humidity, and the vector wind field) between observations and simulations: Luhu urban station (*top*) and the Wanqingsha regional background station (*bottom*)

Table 4 Statistical parameters for the Fifth-Generation Pennsylvania State University/National Center for Atmospheric Research (PSU/NCAR) Mesoscale Model (MM5) performance

Station type	Statistical parameter	Observed mean	Simulated mean	MB	MNB (%)	MNE (%)	*R*
Urban stations	T	22.4	21.3	1.1	4	9	0.76
	P	1,012.2	1,011.0	1.2	0.1	0.2	0.86
	Rh	65.6	71.0	−5.4	−12	17	0.83
Regional background stations	T	21.9	20.8	1.1	4	9	0.75
	P	1,000.9	1,005.2	−4.3	−0.4	0.8	0.87
	Rh	69.3	70.8	−1.5	−7	18	0.83

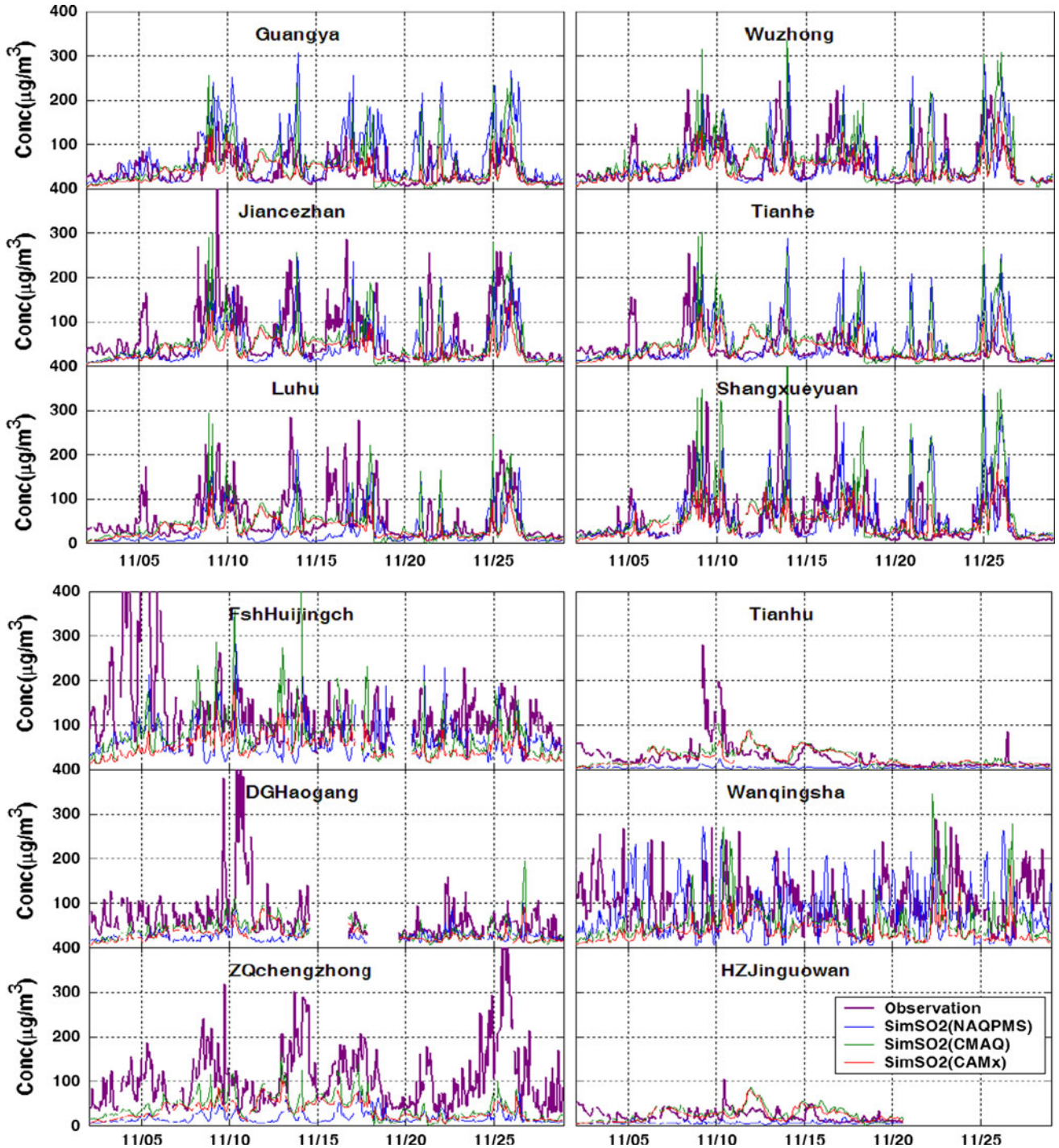

Fig. 6 Time series of SO_2 observations and simulations. The first six stations are in the urban area of Guangzhou, the FshHuijingch, DGHaogang, and ZQchengzhong stations are in the surrounding cities, and the Tianhu, Wanqingsha, and HZJinguowan stations are the background stations in the PRD-RAQM Network

Tianhu and HZJinguowan stations are located in the northern and eastern portions of the PRD region, far away from the major emission sources of that region, so the observed SO_2 concentrations at the two stations are 27.9 and 21.7 μg/m^3, respectively (Table 6), while Wanqingsha station is located at the core of the PRD region, and its observed monthly SO_2 concentration reaches 96.7 μg/m^3. This illustrates that the transport caused by the horizontal advection and diffusion in the NAQPMS model for the regional background SO_2 concentration is not enough; thus, the transport of the NAQPMS model to sites that are far away from the major emission sources (such as Tianhu,

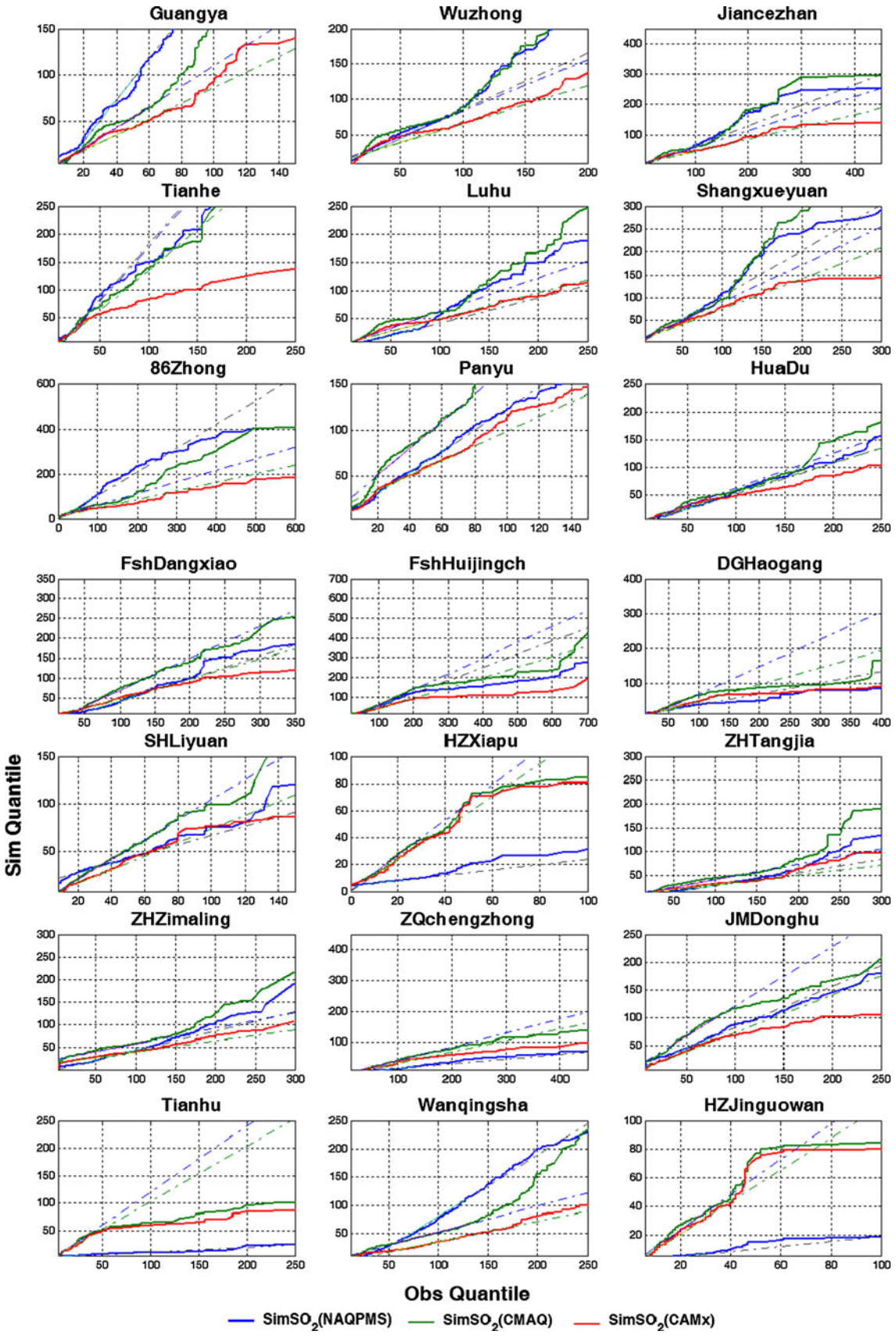
Guangya
Wuzhong
Jiancezhan
Tianhe
Luhu
Shangxueyuan
86Zhong
Panyu
HuaDu
FshDangxiao
FshHuijingch
DGHaogang
SHLiyuan
HZXiapu
ZHTangjia
ZHZimaling
ZQchengzhong
JMDonghu
Tianhu
Wanqingsha
HZJinguowan
Sim Quantile
Obs Quantile
SimSO2(NAQPMS)
SimSO2(CMAQ)
SimSO2(CAMx)

◀ **Fig. 7** Simulation–observation quantile–quantile (Q–Q) plots of SO_2 concentration in Guangzhou and surrounding cities in the PRD region; the concentration unit is μg/m^3. The *x*-axis is the number of observations. The first nine stations are from the GZ-AQM Network, which is located in the urban area of Guangzhou, while the second nine stations are from the PRD-RAQM Network, and the last three stations are the regional background stations

HZJinguowan, and Hzxiapu stations) will greatly underestimate the actual concentration more than the other model results.

Compared to the simulation–observation Q–Q plots of the SO_2 concentrations at the other PRD urban stations, the Q–Q scatters at most Guangzhou stations are closer to the line $y = x$, which suggests perfect model results for the concentration distribution; therefore, the simulations at the Guangzhou stations are better than those in the other PRD cities. But at FshDangxiao, SHLiyuan, and JMDonghu stations, the three model results match well and are close to the line $y = x$. These three stations also have the best statistical measures of any of the other PRD cities in Table 7, so the emissions around these stations may be reasonable.

The statistical measures for the Guangzhou stations are shown in Table 5; the MNB of the NAQPMS model is between −35 and 130%, that of the CMAQ model is −20 to 180%, and that of the CAMx model is −26 to 70%; the CAMx model has the best performance according to this measure. The fraction of predictions within a factor of two of the observations (FAC2) and the normalized mean square error (NMSE) are also selected to evaluate model performance. Except for the NAQPMS model results at Luhu station, the FAC2 at the Guangzhou stations are above 40%, which illustrates that the three models perform quite well at the Guangzhou stations. The NMSE is between 0.746 and 3.004, and most are below 2.000, which suggests that the simulation of SO_2 concentration is reasonable. The CAMx model has the best performance, with the lowest MNB and MNE value at most of the Guangzhou stations. This is because, given reasonable emissions and the same chemical mechanisms, the model bias comes from physical processes, and the horizontal advection/diffusion of the CMAQ/CAMx models is better than the NAQPMS, as mentioned above, while the NAQPMS/CAMx models use the two-way grid nesting technological scheme, which is considered to be better than the one-way scheme used by the CMAQ model.

At most stations in the other PRD cities, except SHLiyuan, HZxiapu, and JMDonghu stations, the simulated SO_2 concentrations are underestimated, with the MNB less than zero, so that SO_2 emissions are likely to be underestimated in these other cities. But these stations (SHLiyuan, HZxiapu, and JMDonghu stations) have a same characteristic that their observed monthly SO_2 concentration is lower than 70 μg/m^3. The MNB of the NAQPMS model is −78 to 43%, that of the CMAQ model is −49 to 68%, and that of the CAMx model is −58 to 27%. There is no obvious advantage in the three model results according to the MNB and MNE values, but the CMAQ model has the lowest NMSE value at most stations. Compared to the statistical measures of the other stations, SHLiyuan and JMDonghu stations have the best FAC2 and NMSE values for each model result. But ZQchengzhong station has the worst FAC2 and NMSE values, either because the emissions have been greatly underestimated or because the station location is too close to the boundary in the model domain. Except for ZQchengzhong station, the FAC2 of the NAQPMS model is in the range 31–74%, that of the CMAQ model is 47–66%, and that of the CAMx model is 41–70%.

3.2.2 *Nitrogen dioxide (NO_2)*

Nitrogen dioxide is a gaseous air pollutant that contributes to the formation of particle pollution and ozone, and the PRD region is one of the areas of highest NO_2 concentration in China as seen from space (Zhang et al. 2007). Because the air pollution of NO_2 also attracts research attention, we include here the model performance for the NO_2 simulations in the PRD region.

As the Q–Q plots in Fig. 9 show, the CMAQ and CAMx model results agree well at the Guangzhou stations but show some differences from the NAQPMS model results, which may be due to their different gas-phase chemical mechanism: the NO_2 concentrations of the NAQPMS model are higher than those of the CMAQ/CAMx models, especially at Guangya, Wuzhong, Jiancezhan, Tianhe, and Luhu stations. These stations are all located west of urban Guangzhou (shown in Fig. 4), and the CMAQ/CAMx model results are closer to the perfect model line $y = x$, especially in the low concentration range, which indicates that the CB-IV gas-phase chemistry may be more appropriate for the simulation of the NO_2 concentration distribution at some urban Guangzhou stations. But at Shangxueyuan, 86zhong, and Panyu stations, the NO_2 concentration distribution of the NAQPMS model is better than that of the CMAQ and CAMx models, according to the Q–Q plots, which indicates that the CBM-Z gas-phase chemistry is better there. The comparison between the CB-IV and the CBM-Z gas-phase chemistry mechanisms in the NAQPMS model is shown in Supplementary material 2. The differences in the gas chemistry mechanisms are not the determining factor for the differences in NO_2 simulation between the NAQPMS model and the CMAQ/CAMx models, but the gas chemistry mechanisms are important in causing the difference in the simulations of the three models.

Table 5 Statistical measures for SO_2 simulation at the Guangzhou stations

Station name		Guangya	Wuzhong	Jiancezhan	Tianhe	Luhu	Shangxueyuan	86Zhong	Panyu	HuaDu	Best num
Mean	Observed	38.5	55.5	65.9	35.4	56.5	54.5	73.7	48.3	56.7	–
	NAQPMS	69.7	**57.0**	46.7	49.2	30.7	**60.5**	**71.9**	62.1	30.0	3
	CMAQ	47.4	61.2	**49.1**	48.1	**42.5**	63.5	49.4	97.3	**35.3**	3
	CAMx	**34.9**	44.7	34.9	**35.5**	31.3	45.5	34.3	**57.3**	29.0	3
MNB	NAQPMS	130%	38%	**−2%**	84%	−35%	85%	76%	92%	−32%	1
	CMAQ	57%	56%	14%	78%	**7%**	95%	25%	180%	**−20%**	2
	CAMx	**27%**	**22%**	−10%	**36%**	−14%	**39%**	**−4%**	**70%**	−26%	6
MNE	NAQPMS	148%	72%	68%	114%	72%	118%	133%	119%	58%	0
	CMAQ	97%	92%	77%	110%	70%	128%	87%	189%	**53%**	1
	CAMx	**76%**	**68%**	**66%**	**71%**	**59%**	**83%**	**71%**	**95%**	54%	8
FAC2	NAQPMS	55%	**71%**	**54%**	61%	30%	**62%**	**46%**	59%	45%	4
	CMAQ	**56%**	58%	49%	53%	**56%**	52%	45%	47%	**57%**	3
	CAMx	55%	61%	46%	**62%**	51%	58%	42%	**61%**	50%	2
NMSE	NAQPMS	1.322	**0.831**	**1.141**	1.602	1.755	1.157	**1.569**	0.803	1.301	3
	CMAQ	1.089	0.984	1.290	1.546	**1.332**	1.448	2.102	1.373	**1.139**	2
	CAMx	**0.746**	0.880	1.874	**1.049**	1.757	**0.961**	3.004	**0.608**	1.674	4

Numbers in **bold** show the best model performance; "Best num" indicates the number of stations for which the model has the best performance

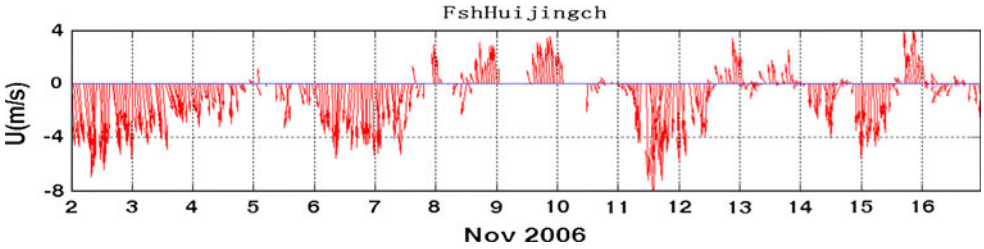

Fig. 8 Observed vector winds at FshHuijingch station in November 2006; the wind on 5 November was calm

Table 6 Statistical measures for SO_2 in the regional background stations

Station name	Wanqingsha			Tianhu			HZJinguowan		
	NAQPMS	CMAQ	CAMx	NAQPMS	CMAQ	CAMx	NAQPMS	CMAQ	CAMx
Observed	96.7			27.9			21.7		
Mean	77.4	58.1	36.1	4.1	26.3	24.5	6.1	26.5	23.8
MB	−19.3	−38.7	−60.6	−23.8	−1.6	−3.5	−15.7	4.8	2.1
FAC2	45%	44%	35%	10%	56%	64%	23%	58%	63%
NMSE	0.834	1.079	2.026	12.624	1.042	1.357	3.251	0.675	0.656

In the other PRD stations, the emissions around Foshan, Dongguan, Shenzhen, and Jiangmen may be reasonable according to the Q–Q plots at FshDangxiao, FshHuijingch, DGHaogang, SHLiyuan, and JMDonghu stations. As shown in Fig. 9, the model results are a little lower than the observations at these stations. But at SHLiyuan Station, the NO_2 concentrations of the NAQPMS model are much higher than those of the CMAQ/CAMx models, and higher than the observations in the high concentration range. The Q–Q plots of the ZHTangjia, ZHZimaling, and ZQchengzhong stations show another pattern, with the Q–Q scattering all below the line $y = x$; thus, the simulations are lower than the observations throughout the whole concentration range. There is a reason for why the emissions, which can deplete NO_2 concentration, may be underestimated. Unfortunately, at HZXiapu station, the Q–Q scatters of the three model results are much closer to the x-axis, so that the model results are near zero; this reason needs more analysis and model testing.

As with the SO_2 concentration, the performance of the CMAQ/CAMx models for NO_2 concentration is better in the regional background stations at Tianhu and

Table 7 Statistical measures for SO_2 simulations in other the PRD urban stations

Station name		FshDangxiao	FshHuijingch	DGHaogang	SHLiyuan	HZXiapu	ZHTangjia	ZHZimaling	ZQchengzhong	JMDonghu
Mean	Observed	95.5	126.8	65.5	33.5	20.7	84.1	80.4	104.3	63.9
	NAQPMS	43.7	66.7	26.0	35.5	7.7	26.6	36.1	18.1	56.8
	CMAQ	70.5	75.8	38.1	36.0	22.1	38.8	53.4	41.3	78.0
	CAMx	47.7	50.4	29.4	27.4	20.3	27.8	36.2	32.5	47.1
MNB	NAQPMS	−44%	−32%	−45%	43%	−47%	−48%	−13%	−78%	23%
	CMAQ	**−7%**	**−21%**	**−21%**	36%	34%	**−18%**	31%	**−49%**	68%
	CAMx	−36%	−46%	−36%	**4%**	**27%**	−42%	**−10%**	−58%	**4%**
MNE	NAQPMS	59%	**51%**	55%	69%	**57%**	**70%**	86%	79%	61%
	CMAQ	57%	56%	**53%**	71%	79%	67%	92%	**58%**	90%
	CAMx	**53%**	55%	55%	**52%**	74%	61%	**74%**	63%	**60%**
FAC2	NAQPMS	38%	**53%**	40%	**73%**	38%	31%	35%	6%	**74%**
	CMAQ	**62%**	52%	**58%**	64%	53%	**47%**	**48%**	**36%**	66%
	CAMx	47%	41%	48%	70%	**55%**	41%	42%	25%	64%
NMSE	NAQPMS	1.389	1.411	2.473	**0.482**	2.247	3.267	1.587	6.344	0.484
	CMAQ	**0.628**	**1.335**	**1.510**	0.679	**0.804**	**2.152**	**0.925**	**2.027**	**0.471**
	CAMx	1.136	2.433	2.260	0.708	0.872	3.213	1.744	2.928	0.700

Numbers in **bold** show the best model performance

Table 8 Statistical measures for NO_2 at the Guangzhou stations

Station name		Guangya	Wuzhong	Jiancezhan	Tianhe	Luhu	Shangxueyuan	86Zhong	Panyu	HuaDu	Best num
	Observed	92.3	78.4	94.1	96.4	72.1	68.7	84.6	71.1	47.5	–
MNB	NAQPMS	88%	126%	60%	54%	**5%**	40%	**−8%**	26%	**−20%**	3
	CMAQ	**−46%**	11%	**−46%**	**−45%**	−50%	**−7%**	−55%	**−6%**	−49%	5
	CAMx	−59%	**10%**	−56%	−51%	−67%	−20%	−72%	−38%	−67%	1
MNE	NAQPMS	105%	140%	77%	82%	69%	68%	**46%**	55%	**46%**	2
	CMAQ	**51%**	41%	**51%**	**49%**	**60%**	44%	58%	**39%**	54%	5
	CAMx	62%	**40%**	58%	53%	71%	**42%**	72%	49%	69%	2
FAC2	NAQPMS	**57%**	48%	**69%**	**59%**	**54%**	68%	**71%**	**77%**	**62%**	7
	CMAQ	44%	**87%**	44%	47%	32%	**70%**	35%	**77%**	42%	3
	CAMx	26%	84%	31%	38%	16%	67%	11%	53%	16%	0
NMSE	NAQPMS	0.965	0.820	**0.619**	**0.547**	**0.728**	**0.456**	**0.447**	**0.289**	**0.655**	7
	CMAQ	**0.792**	**0.261**	0.710	0.790	1.262	0.457	1.560	0.296	1.036	2
	CAMx	1.370	0.313	1.166	1.040	2.615	0.666	3.325	0.811	2.610	0

Numbers in **bold** show the best model performance

HZJinguowan, which are far away from major emission sources, and the NAQPMS model results are better at Wanqingsha Station. The transport of the NO_2 concentration in the NAQPMS model is also underestimated more than in the other two models.

Statistical parameters (MNB, MNE, FAC2, and NMSE) are also calculated for model evaluation in Tables 8 and 9. The MNB of the NAQPMS model in Guangzhou is between −20 and 126% and is overestimated at most stations. But the CMAQ and CAMx models are mostly underestimated, with MNB values ranging from −55 to 11% and from −67 to 10%, respectively. Comparing the MNE of the three models, the CMAQ model has the best model bias, with an MNE of 39–60%. The NAQPMS model has the lowest NMSE value at most stations. For FAC2, the most robust measure because it is not overly influenced by outliers (Chang and Hanna 2004), the NAQPMS model has the best performance, with an average FAC2 of 63%, compared with CMAQ (53%) and CAMx (38%). Thus the NAQPMS model has the best performance at the Guangzhou stations, which may be because the NAQPMS model includes the CBM-Z gas-phase chemical mechanism, and this may be better than the CMAQ/CAMx models' CB-IV gas-phase mechanism at

Table 9 Statistical measures for NO_2 simulations in the other PRD cities stations

Sta Name		FshDangxiao	FshHuijingch	DGHaogang	SHLiyuan	HZXiapu	ZHTangjia	ZHZimaling	ZQchengzhong	JMDonghu
	Observed	73.4	89.9	65.3	86.7	50.1	73.6	83.8	58.3	44.2
MNB	NAQPMS	−27%	14%	11%	40%	−59%	−69%	−59%	−86%	52%
	CMAQ	−15%	−25%	−19%	−31%	−80%	−50%	−39%	−71%	68%
	CAMx	−41%	−33%	−32%	−38%	−86%	−71%	−63%	−84%	4%
MNE	NAQPMS	61%	53%	53%	83%	65%	74%	64%	86%	79%
	CMAQ	46%	33%	41%	39%	82%	65%	55%	75%	89%
	CAMx	52%	39%	49%	41%	86%	75%	71%	85%	64%
FAC2	NAQPMS	44%	71%	70%	53%	27%	19%	28%	3%	70%
	CMAQ	65%	76%	74%	64%	7%	32%	44%	19%	65%
	CAMx	46%	67%	54%	59%	5%	15%	18%	7%	57%
NMSE	NAQPMS	1.174	0.432	0.452	0.540	5.487	2.810	2.018	7.203	0.451
	CMAQ	0.515	0.407	0.423	0.435	10.07	1.659	0.934	2.304	0.392
	CAMx	1.079	0.590	0.753	0.535	16.38	3.753	2.333	5.809	0.715

the Guangzhou stations. The gas-phase chemistry mechanism plays an important role in simulating the photochemistry reaction involving NOx-O_3-VOCs.

Except for JMDonghu Station, the NO_2 simulations of the other PRD cities stations are underestimated, with their MB being less than zero, ranging from −8.1 μg/m^3 (the NAQPMS model results at FshHuijingchen station) to −58.9 μg/m^3 (the CAMx model results at ZHZimaling Station). Thus, the MNB of the three models at most stations is less than zero, and the NOx emissions in the other PRD cites might be underestimated. The CMAQ model has the best model bias according to the MNE value (33–82%), compared with the NAQPMS model's 53–86% and the CAMx model's 39–86%. The average FAC2 of the three models are 43, 50, and 36%, respectively; here, also, the CMAQ model results are the best. For the measure of NMSE, the CMAQ is in the range 0.392–10.07 with an average of 1.905, the NAQPMS is in the range 0.432–7.203 with an average of 2.285, and the CAMx is 0.590–16.38 with an average of 3.550. Thus, the CMAQ model has the best performance in NO_2 simulations in the other PRD cities stations.

3.2.3 *Respirable suspended particulates (PM_{10})*

The PM_{10} not only comes from a great variety of primary emissions sources, including fugitive dust and industrial source emissions, but is also produced by the oxidization of gaseous pollutants or in photochemical reactions as a secondary aerosol. Thus, the calculation of the PM_{10} concentration includes several species in the models, and the equation is shown as follows.

In the CMAQ model, we derive the PM_{10} concentration according to Byun and Ching (1999) and Binkowski and Roselle (2003):

$$\begin{aligned}\mathrm{PM10} = {} & \mathrm{ASO_4} + \mathrm{ANH_4} + \mathrm{ANO_3} + \mathrm{AORGA} \\ & + \mathrm{AORGPA} + \mathrm{AORGB} + \mathrm{AEC} + \mathrm{A25} + \mathrm{ACORS} \\ & + \mathrm{ASEAS} + \mathrm{ASOIL}\end{aligned}$$

In the CAMx model (ENVIRON 2002):

$$\begin{aligned}\mathrm{PM10} = {} & \mathrm{PSO_4} + \mathrm{PNO_3} + \mathrm{PNH_4} + \mathrm{POA} + \mathrm{PEC} + \mathrm{FCRS} \\ & + \mathrm{CCRS} + \mathrm{FPRM} + \mathrm{CPRM} + \mathrm{SOA1} \\ & + \mathrm{SOA2} + \mathrm{SOA3} + \mathrm{SOA4} + \mathrm{SOA5}\end{aligned}$$

And in the NAQPMS model (Wang et al. 2006b; Wu et al. 2010b):

$$\begin{aligned}\mathrm{PM10} = {} & \mathrm{POA} + \mathrm{PEC} + \mathrm{PM25} + \mathrm{PMC} \\ & + \mathrm{SO_4} + \mathrm{NO_3} + \mathrm{NH_4}\end{aligned}$$

The model performance for PM_{10} concentrations has also been evaluated with Q–Q plots and statistical parameters. At most of the Guangzhou stations, the model PM_{10} concentrations are in agreement with the observations. But at Guangya and Tianhe stations, the NAQPMS model results are overestimated throughout the whole concentration distribution, while the CMAQ/CAMx model results are better according to the Q–Q plots in Fig. 10. At Wuzhong Station, all three model results are overestimated, while the Q–Q scatters are all above the line $y = x$, with an MNB of 160–215% (Table 10). Thus, the PM_{10}-related emissions around Wuzhong station might be overestimated. In contrast, the PM_{10}-related emissions may be underestimated at 86Zhong and HuaDu stations, since the Q–Q scatters are much below the line $y = x$, with an MNB of −29 to −12% and −34 to −27%, respectively. The Q–Q plots at Luhu and Jiancezhan stations show another pattern, with simulations that are satisfactory in the low concentration range, but overestimated in the high concentration range. In other words, the CMAQ/CAMx

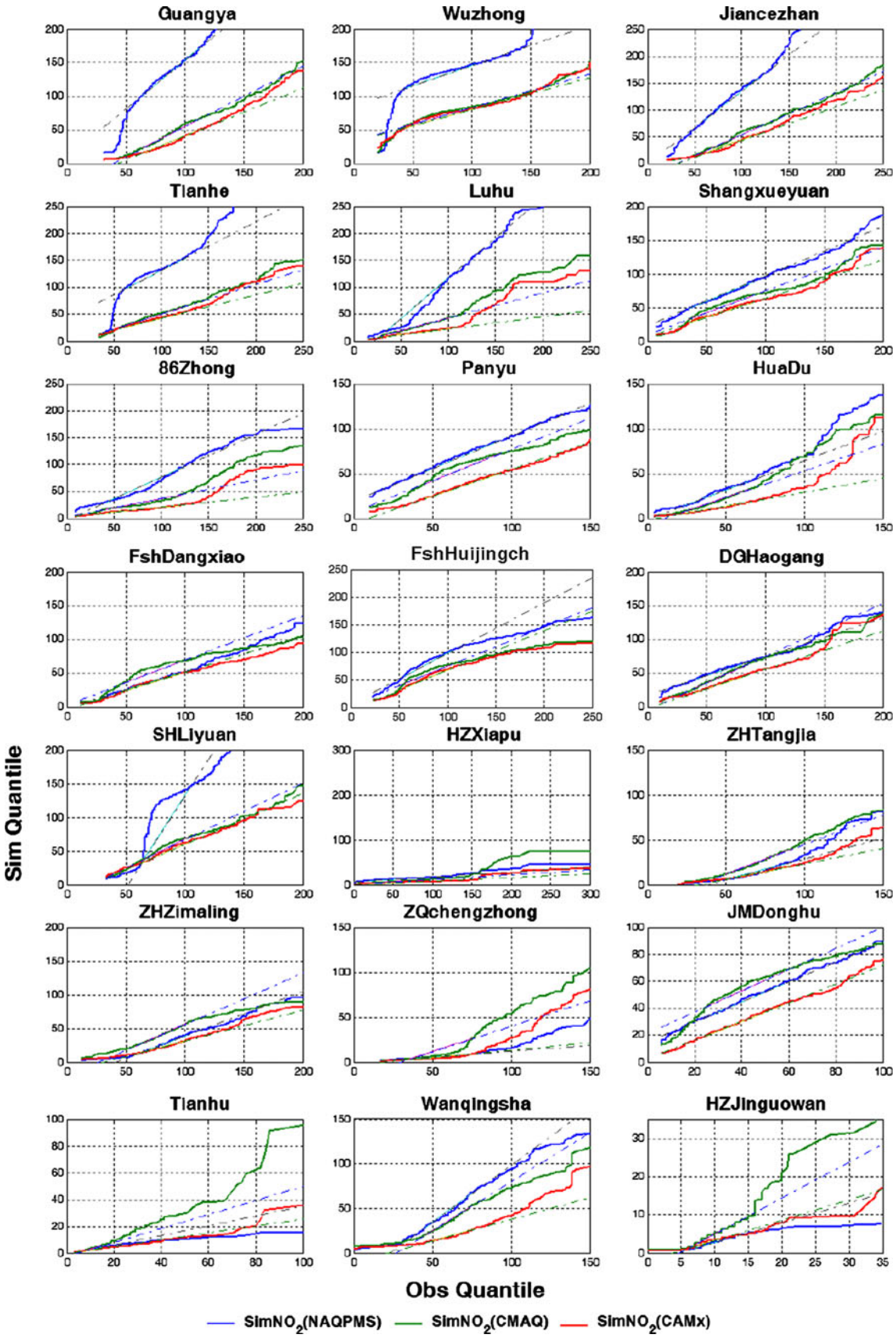

Fig. 9 Same as Fig. 7, but for NO_2 concentration

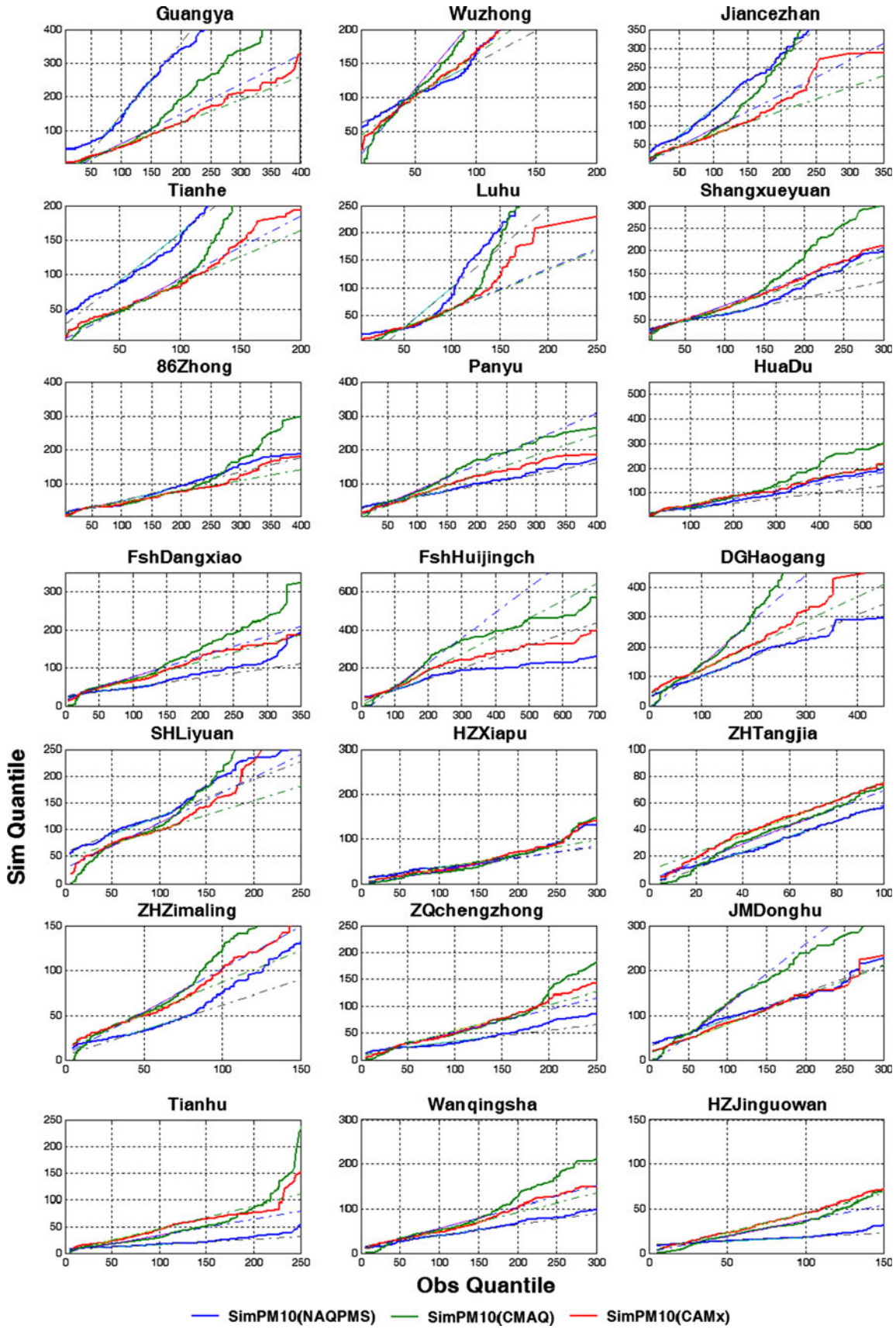

Fig. 10 Same as Fig. 7, but for PM_{10}. The concentration unit is $\mu g/m^3$

Table 10 Statistical parameters of the three model performances for PM_{10} concentration

Sta name	Guangya	Wuzhong	Jiancezhan	Tianhe	Luhu	Shangxueyuan	86Zhong	Panyu	HuaDu
Mean									
Observed	118.4	69.8	88.8	78.0	79.1	100.0	127.4	114.1	104.6
NAQPMS	180.3	131.7	130.3	131.3	72.3	68.5	61.0	67.5	40.2
CMAQ	86.8	165.1	95.4	84.1	58.4	86.9	59.7	90.9	49.0
CAMx	67.6	131.6	72.4	73.8	51.5	78.4	53.5	72.7	49.8
MNB									
NAQPMS	92%	188%	166%	150%	4%	30%	−12%	−3%	−34%
CMAQ	−18%	215%	68%	44%	−17%	42%	−21%	16%	−32%
CAMx	−32%	160%	35%	31%	−22%	31%	−29%	−6%	−27%
FAC2									
NAQPMS	59%	51%	55%	57%	52%	47%	41%	55%	48%
CMAQ	51%	40%	56%	64%	54%	55%	39%	64%	49%
CAMx	57%	50%	59%	70%	61%	60%	38%	59%	52%
NMSE									
NAQPMS	0.832	0.956	0.823	0.747	0.620	0.907	1.586	0.876	2.513
CMAQ	0.892	1.980	0.920	0.648	0.739	0.687	1.624	0.551	1.557
CAMx	0.873	0.931	0.568	0.369	0.581	0.586	1.780	0.738	1.530

Table 11 Comparison of model performance measures between the Guangzhou stations and the other PRD cities stations

Species	Statistical parameter	Guangzhou stations			Other PRD cities stations		
		Maximum	Minimum	Average	Maximum	Minimum	Average
SO_2	MNB	180%	−35%	40%	68%	−78%	−14%
	FAC2	71%	30%	53%	74%	6%	48%
	NMSE	3.004	0.608	1.346	6.344	0.471	1.711
NO_2	MNB	126%	−72%	−13%	68%	−86%	−33%
	FAC2	87%	11%	51%	76%	3%	43%
	NMSE	3.325	0.261	0.985	16.387	0.392	2.580
PM_{10}	MNB	215%	−34%	38%	115%	−65%	18%
	FAC2	70%	38%	53%	78%	17%	56%
	NMSE	2.513	0.369	1.015	2.497	0.341	0.904

model results are better than those of the NAQPMS model at the Guangzhou stations.

There are also three patterns in the Q–Q plots of the other PRD cities stations. In the first pattern, which appears at HZXiapu, ZHTangjia, and ZQchengzhong stations, the Q–Q scatters are all below the line $y = x$ throughout the concentration range. In the second pattern, the Q–Q scatters are a little lower than the line $y = x$, especially in the high concentration range, as shown at the Foshan City stations, including FshDangxiao and FshHuijingchen stations. Thus, the highly elevated source emissions in Foshan might be somewhat underestimated. This is because high PM_{10} concentration events usually occur during times of weak winds, so the local highly elevated source emissions would contribute more PM_{10} concentration. In the last pattern, the simulations match the observations well and the Q–Q scatters are close to the perfect model line $y = x$, such as at SHLiyuan and JMDonghu stations.

The FAC2 of the three models in Guangzhou is 41–59, 39–64, and 38–70%, respectively, while in the other PRD cities stations, it is 27–78, 17–71, and 28–74%. Therefore, the PM_{10} simulations in Guangzhou are a little better than those at the other PRD stations.

Among the three pollutants, the PM_{10} model results have the best measures of FAC2 and NMSE, as shown in Table 11, but this simulation is greatly overestimated at some stations, such as Wuzhong Station, as shown in Table 10.

The model performance of SO_2 and NO_2 simulations at the Guangzhou stations is better than that at the other PRD cities stations, with better FAC2 and NMSE values, as shown in Table 11. But the SO_2 and NO_2 emissions in the other PRD cities might be more underestimated, because the maximum/minimum and average MNB of the three

model results in the other PRD cities stations are lower than those at the Guangzhou stations.

4 Conclusions

The Nested Air Quality Prediction Modeling System (NAQPMS), Community Multiscale Air Quality (CMAQ), and Comprehensive Air Quality Model with extensions (CAMx) air quality models are evaluated with the same meteorological fields and the same emissions data for a 1-month-long simulation over the Pearl River Delta (PRD) region. The meteorological fields, generated from the Fifth-Generation Pennsylvania State University/National Center for Atmospheric Research (PSU/NCAR) Mesoscale Model (MM5), match well with the observations in the regional background monitoring stations, and the meteorological simulations are reasonable for this air quality simulation study. The emissions data includes the regional emission inventories from Transport and Chemical Evolution over the Pacific/Intercontinental Chemical Transport ExperimentPhase B (TRACE-P/INTEX-B) and the local emission inventories, which are processed by the Sparse Matrix Operator Kernel Emissions (SMOKE) model as area/point sources for the air quality models.

The air quality models show different advantages at different stations. The CAMx model has the best performance in SO_2 simulation, with the lowest mean normalized bias (MNB) and mean normalized error (MNE) at most of the Guangzhou stations, while the CMAQ model has the lowest normalized mean square error (NMSE) value for SO_2 simulation in most of the other PRD cities stations. The Nested Air Quality Prediction Modeling System (NAQPMS) model has the best performance in NO_2 simulation at most of the Guangzhou stations, but at some western urban stations in Guangzhou, the CMAQ/CAMx model results are better. This could be because the CBM-Z gas-phase mechanism is better than the CB-IV mechanism at the Guangzhou stations. The SO_2 and NO_2 simulations of the NAQPMS model are lower and worse than those of the CMAQ/CAMx models at Tianhu and Hzjinguowan stations, but they are better than the CMAQ/CAMx models at Wanqingsha Station, which illustrates that the transport caused by the horizontal advection and diffusion of the NAQPMS model is lower than that of the CMAQ/CAMx models.

The model performance at the Guangzhou stations is better than that at the other PRD cities stations, which might be due to the more detailed emission inventories which we obtained in Guangzhou. Also, emissions may be underestimated in the other PRD cities. Thus, the modeled SO_2/NO_2 concentrations are underestimated more in the other PRD cities urban stations, and the maximum/minimum and average MNB of the three models at the other PRD cities stations are lower than those at the Guangzhou stations.

Among the three species, the PM_{10} simulations yielded the best model measures of FAC2 (fraction of predictions within a factor of two of the observations) and NMSE, and the SO_2 simulation showed the best concentration distribution, with most simulation–observation quantile–quantile (Q–Q) plot scatters being close to the line $y = x$.

Acknowledgments This work is supported by the National High Technology Research and Development Program of China (No. 2010AA012305) and Hong Kong ECF project 9211008.

Appendices

The normalized mean square error (NMSE): $\mathrm{NMSE} = \frac{\left(C_o - C_p\right)^2}{C_o \times C_p}$

FAC2 (fraction of predictions within a factor of two of the observations) = fraction of data that satisfies: $0.5 \leq \frac{C_p}{C_o} \leq 2$

References

An X, Zhu T, Wang Z, Li C, Wang Y (2007) A modeling analysis of a heavy air pollution episode occurred in Beijing. Atmos Chem Phys 7:3103–3114. doi:10.5194/acp-7-3103-2007

Binkowski FS, Roselle SJ (2003) Models-3 community multiscale air quality (CMAQ) model aerosol component 1. Model description. J Geophys Res Atmos 108(D6):4183. doi:10.1029/2001JD001409

Byun DW, Ching JKS (1999) Science algorithms of the EPA Models-3 Community Multi-scale Air Quality (CMAQ) Modeling System. EPA/600/R-99/030. National Exposure Research Laboratory, U.S. Environmental Protection Agency, Research Triangle Park, NC. Available online at: http://www.epa.gov/AMD/CMAQ/000_cover_exec.pdf

Byun D, Schere KL (2006) Review of the governing equations, computational algorithms, and other components of the Models-3 Community Multiscale Air Quality (CMAQ) modeling system. Appl Mech Rev 59(1–6):51–77

Chan CK, Yao XH (2008) Air pollution in mega cities in China. Atmos Environ 42(1):1–42

Chang JC, Hanna SR (2004) Air quality model performance evaluation. Meteorol Atmos Phys 87:167–196

Chen XL, Feng YR, Li JN, Lin WS, Fan SJ, Wang AY, Fong SK, Lin H (2009) Numerical simulations on the effect of sea-land breezes on atmospheric haze over the Pearl River Delta region. Environ Model Assess 14(3):351–363

Cheng SY, Chen DS, Li JB, Wang HY, Guo XR (2007) The assessment of emission-source contributions to air quality by using a coupled MM5-ARPS-CMAQ modeling system: a case study in the Beijing metropolitan region, China. Environ Model Softw 22(11):1601–1616

Colle BA, Westrick KJ, Mass CF (1999) Evaluation of MM5 and Eta-10 precipitation forecasts over the Pacific Northwest during the cool season. Weather Forecast 14:137–156

Cruickshank TS (2008) CMAQ sensitivity to winter-time ground surface albedo. In: Proceedings of the 7th Annual Community

Modeling and Analysis (CMAS) Conference: Model Evaluation and Analysis, Chapel Hill, NC, October 2008

Demerjian KL, Schere KL, Peterson JT (1980) Theoretical estimates of actinic (spherically integrated) flux and photolytic rate constants of atmospheric species in the lower troposphere. Adv Environ Sci Tech 10:369–459

Deng XJ, Tie XX, Zhou XJ, Wu D, Zhong LJ, Tan HB, Li F, Huang XY, Bi XY, Deng T (2008) Effects of Southeast Asia biomass burning on aerosols and ozone concentrations over the Pearl River Delta (PRD) region. Atmos Environ 42(36):8493–8501

ENVIRON (2002) User's guide to the Comprehensive Air Quality Modeling System with Extensions (CAMx), version 4.4.. ENVIRON International Corporation, Novato, CA, pp 10, 16, 29, 30, 38–40

Feng YR, Wang AY, Wu D, Xu XD (2007) The influence of tropical cyclone Melor on PM_{10} concentrations during an aerosol episode over the Pearl River Delta region of China: numerical modeling versus observational analysis. Atmos Environ 41(21):4349–4365

Guangdong ProvincialEnvironmental ProtectionMonitoring Centre (GDEMC), Hong Kong Environmental Protection Department (HKEPD) (2007) Pearl River Delta regional air quality monitoring network: a report of monitoring results in 2006, pp 1–15. http://www.epd.gov.hk/epd/english/resources_pub/publications/files/PRD_2006_report_en.pdf

Guangdong ProvincialEnvironmental ProtectionMonitoring Centre (GDEMC), Hong Kong Environmental Protection Department (HKEPD) (2009) Pearl River Delta regional air quality monitoring network: a report of monitoring results for the period between January and June 2009, pp 1–10. http://www.epd.gov.hk/epd/english/resources_pub/publications/files/PRD2009_1-6e.pdf

Gery MW, Whitten GZ, Killus JP, Dodge MC (1989) A photochemical kinetics mechanism for urban and regional scale computer modeling. J Geophys Res Atmos 94(D10):12.925–12.956

Grell GA, Dudhia J, Stauffer DR (1994) A description of the fifth-generation Penn State/NCAR Mesoscale Model (MM5). NCAR Technical Note NCAR/TN-398+ STR. National Center for Atmospheric Research (NCAR), Boulder, CO

Houyoux MR, Vukovich JM (1999) Updates to the Sparse Matrix Operator Kernel Emissions (SMOKE) Modeling System and Integration with Models-3. Environmental Programs MCNC, North Carolina Supercomputing Center, 3021 Cornwallis Road, Research Triangle Park, NC, 27709–2889

Huang MY, Wang ZF, He DY, Xu HY, Zhou L (1995) Modeling studies on sulfur deposition and transport in East Asia. Water Air Soil Pollut 85(4):1921–1926

Li J, Wang ZF, Akimoto H, Gao C, Pochanart P, Wang X (2007) Modeling study of ozone seasonal cycle in lower troposphere over east Asia. J Geophys Res 112(D22S25). doi:10.1029/2006JD008209

Lo JCF, Lau AKH, Chen F, Fung JCH, Leung KKM (2007) Urban modification in a mesoscale model and the effects on the local circulation in the Pearl River Delta region. J Appl Meteor Climatol 46:457–476

Madronich S (2002) Tropospheric Ultraviolet and Visible (TUV) Radiation Model. National Center for Atmospheric Research (NCAR), Boulder, CO. Home page at: http://www.acd.ucar.edu/TUV/

Padro J, den Hartog G, Neumann HH (1991) An investigation of the ADOM dry deposition module using summertime O_3 measurements above a deciduous forest. Atmos Env Part A General Topics 25(8):1689–1704

Seinfeld JH, Pandis SN (1998) Atmospheric chemistry and physics: from air pollution to climate change. John Wiley & Sons, Inc., New York

Strader R, Lurmann F, Pandis SN (1999) Evaluation of secondary organic aerosol formation in winter. Atmos Environ 33:4849–4863

Streets DG, Bond TC, Carmichael GR, Fernandes SD, Fu Q, He D, Klimont Z, Nelson SM, Tsai NY, Wang MQ, Woo J-H, Yarber KF (2003) An inventory of gaseous and primary aerosol emissions in Asia in the year 2000. J Geophys Res 108(D21):8809. doi:10.1029/2002JD003093

Streets DG, Zhang Q, Wang LT, He KB, Hao JM, Wu Y, Tang YH, Carmichael GR (2006) Revisiting China's CO emissions after the Transport and Chemical Evolution over the Pacific (TRACE-P) mission: synthesis of inventories, atmospheric modeling, and observations. J Geophys Res Atmos 111(D14306). doi:10.1029/2006JD007118

Tesche TW, Morris R, Tonnesen G, McNally D, Boylan J, Brewer P (2006) CMAQ/CAMx annual 2002 performance evaluation over the eastern US. Atmos Environ 40(26):4906–4919

Walcek CJ, Aleksic NM (1998) A simple but accurate mass conservative, peak-preserving, mixing ratio bounded advection algorithm with FORTRAN code. Atmos Environ 32:3863–3880

Wang ZF, Sha WM, Ueda H (2000) Numerical modeling of pollutant transport and chemistry during a high-ozone event in northern Taiwan. Tellus B 52(5):1189–1205

Wang ZF, Maeda T, Hayashi M, Hsiao L-F, Liu K-Y (2001) A nested air quality prediction modeling system for urban and regional scales: application for high-ozone episode in Taiwan. Water Air Soil Pollut 130:391–396

Wang ZF, Akimoto H, Uno I (2002) Neutralization of soil aerosol and its impact on the distribution of acid rain over east Asia: observations and model results. J Geophys Res 107(D19):4389

Wang XM, Carmichael G, Chen DL, Tang YH, Wang TJ (2005) Impacts of different emission sources on air quality during March 2001 in the Pearl River Delta (PRD) region. Atmos Environ 39(29):5227–5241

Wang Z-F, Xie F-Y, Wang X-Q, An J-L, Zhu J (2006a) Development and application of nested air quality prediction modeling system. Chin J Atmos Sci 30:778–790 (in Chinese)

Wang ZF, Li J, Wang XQ, Pochanart P, Akimoto H (2006b) Modeling of regional high ozone episode observed at two mountain sites (Mt. Tai and Huang) in East China. J Atmos Chem 55(3):253–272

Wang W, Ren LH, Zhang YH, Chen JH, Liu HJ, Bao LF, Fan SJ, Tang DG (2008) Aircraft measurements of gaseous pollutants and particulate matter over Pearl River Delta in China. Atmos Environ 42(25):6187–6202

Wang XM, Chen F, Wu ZY, Zhang MG, Tewari M, Guenther A, Wiedinmyer C (2009a) Impacts of weather conditions modified by urban expansion on surface ozone: comparison between the Pearl River Delta and Yangtze River Delta regions. Adv Atmos Sci 26(5):962–972

Wang ZF, Wu QZ, Gbaguidi AE, Yan PZ, Zhang W, Wang W, Tang X (2009b) Ensemble air quality multi-model forecast system for Beijing (EMS-Beijing): model description and preliminary application. J Nanjing University Inform Sci Technol: Natural Science Edition 1(1):19–26 (in Chinese)

Wu QZ, Wang ZF, Xu WS, Huang JP, Gbaguidi A (2010a) Multi-model simulation of PM_{10} during the 2008 Beijing Olympic Games: effectiveness of emission restrictions. Acta Scientiae Circumstantiae 30(9):1739–1748 (in Chinese)

Wu QZ, Wang ZF, Gbaguidi A, Tang X, Zhou W (2010b) Numerical study of the effect of traffic restriction on air quality in Beijing. SOLA 6A:17–20. doi:10.2151/sola.6A-005

Wu QZ, Wang ZF, Gbaguidi A, Gao C, Li LN, Wang W (2011) A numerical study of contributions to air pollution in Beijing during CAREBeijing-2006. Atmos Chem Phys 11:5997–6011. doi:10.5194/acp-11-5997-2011

Zaveri RA, Peters LK (1999) A new lumped structure photochemical mechanism for large-scale applications. J Geophys Res 104(D23):30387–30415

Zhang MG, Uno I, Zhang RJ, Han ZW, Wang ZF, Pu YF (2006) Evaluation of the Models-3 Community Multi-scale Air Quality (CMAQ) modeling system with observations obtained during the TRACE-P experiment: comparison of ozone and its related species. Atmos Environ 40(26):4874–4882

Zhang Q, Streets DG, He KB, Wang YX, Richter A, Burrows JP, Uno I, Jang CJ, Chen D, Yao ZL, Lei Y (2007) NOx emission trends for China, 1995–2004: the view from the ground and the view from space. J Geophys Res Atmos 112(D22306). doi:10.1029/2007JD008684

Zhang YH, Hu M, Zhong LJ, Wiedensohler A, Liu SC, Andreae MO, Wang W, Fan SJ (2008) Regional integrated experiments on air quality over Pearl River Delta 2004 (PRIDE-PRD2004): overview. Atmos Environ 42(25):6157–6173

Zhang Q, Streets DG, Carmichael GR, He KB, Huo H, Kannari A, Klimont Z, Park IS, Reddy S, Fu JS, Chen D, Duan L, Lei Y, Wang LT, Yao ZL (2009) Asian emissions in 2006 for the NASA INTEX-B mission. Atmos Chem Phys 9(14):5131–5153

Zheng JY, Zhang LJ, Che WW, Zheng ZY, Yin SS (2009) A highly resolved temporal and spatial air pollutant emission inventory for the Pearl River Delta region, China and its uncertainty assessment. Atmos Environ 43(32):5112–5122

Zhou W, Wang X, Zhou TJ, Li CY, Chan JCL (2007a) Interdecadal variability of the relationship between the East Asian winter monsoon and ENSO. Meteorol Atmos Phys 98:283–293. doi:10.1007/s00703-007-0263-6

Zhou W, Li CY, Wang X (2007b) Possible connection between Pacific oceanic interdecadal pathway and East Asian winter monsoon. Geophys Res Lett 34(L01701). doi:10.1029/2006GL027809

Zhou W, Chan JCL, Chen W, Ling J, Pinto JG, Shao YP et al (2009) Synoptic-scale controls of persistent low temperature and icy weather over southern China in January 2008. Mon Wea Rev 137:3978–3991. doi:10.1175/2009MWR2952.1